SJSS SPANISH JOURNAL OF SOIL SCIENCE | SECS SOCIEDAD ESPAÑOLA DE LA CIENCIA DEL SUELO

ORIGINAL RESEARCH
published: 06 April 2023
doi: 10.3389/sjss.2023.11192

Mercury Content and Pools in Complex Polycyclic Soils From a Mountainous Area in Galicia (NW Iberian Peninsula)

Antía Gómez-Armesto[1,2]*, *Melissa Méndez-López*[1,2], *Andrea Parente-Sendín*[1,2], *Noemi Calvo-Portela*[1,2], *Xabier Pontevedra-Pombal*[3], *Eduardo García-Rodeja*[3], *Flora Alonso-Vega*[1,2] and *Juan Carlos Nóvoa-Muñoz*[1,2]*

[1]Área de Edafoloxía e Química Agrícola, Departamento de Bioloxía Vexetal e Ciencia do Solo, Facultade de Ciencias, Universidade de Vigo, Ourense, Spain, [2]Environmental Technology and Assessment Laboratory, Campus da Auga—Campus of Ourense, University of Vigo, Ourense, Spain, [3]Departamento de Edafoloxía e Química Agrícola, Facultade de Bioloxía, Universidade de Santiago de Compostela, Santiago de Compostela, Spain

Atmospheric mercury (Hg) usually tends to accumulate in the upper horizons of soils. However, the physico-chemical characteristics of some soils, as well as pedogenetic processes, past climate changes, or soil degradation processes, can lead to a redistribution of mercury through the soil profile. In this work, the presence and accumulation of mercury was studied in three deep polycyclic soils from a mountainous area in NW Iberia Peninsula. The highest total Hg values (Hg_T) were found in the organic matter-rich O and A horizons of FL and MF profiles (169 and 139 $\mu g\,kg^{-1}$, respectively) and in the illuvial horizon of RV (129.2 $\mu g\,kg^{-1}$), with the latter two samples showing the maximum Hg reservoirs (29.3 and 29.0 $mg\,m^{-2}$, respectively). Despite finding the highest Hg content in the surface horizons, considerable Hg reservoirs were also observed in depths higher than 40–50 cm, indicating the importance of taking into account these soil layers when Hg pools are evaluated at a global scale. Based on the mass transfer coefficients, we can rule out the contribution of parent material to the Hg accumulation in most of the horizons, thus indicating that pedogenetic processes are responsible for the Hg redistribution observed along the soil profiles. Finally, by means of principal component analysis (PCA) and stepwise linear regression we could assess the main soil components involved in the Hg accumulation in each soil horizon. Therefore, PC1 (organic matter and low stability Al-hummus complexes) showed a higher influence on the surface horizons, whereas PC2 (reactive Al-Fe complexes and medium-high Al-hummus complexes) and PC4 (crystalline Fe compounds and pH_w) were more relevant in the Hg distribution observed in the deepest soil layers.

Keywords: soil organic matter, Hg storage, Hg vertical patterns, pedogenetic processes, Al and Fe compounds

OPEN ACCESS

Edited by:
Avelino Núñez-Delgado, University of Santiago de Compostela, Spain

***Correspondence:**
Antía Gómez-Armesto
angomez@uvigo.es
Juan Carlos Nóvoa-Muñoz
edjuanca@uvigo.gal

Received: *12 January 2023*
Accepted: *02 March 2023*
Published: *06 April 2023*

Citation:
Gómez-Armesto A, Méndez-López M, Parente-Sendín A, Calvo-Portela N, Pontevedra-Pombal X, García-Rodeja E, Alonso-Vega F and Nóvoa-Muñoz JC (2023) Mercury Content and Pools in Complex Polycyclic Soils From a Mountainous Area in Galicia (NW Iberian Peninsula). Span. J. Soil Sci. 13:11192. doi: 10.3389/sjss.2023.11192

INTRODUCTION

Hg is a global pollutant of environmental concern, which can cause serious damage to the health of both humans and wildlife, especially in the methylated form (Clarkson and Magos, 2006; Driscoll et al., 2013). Hg is mainly emitted to the atmosphere by both natural and anthropogenic sources and transported far away from its emission point. Therefore, one of the biggest Hg reservoirs in the biosphere is the atmosphere (Obrist et al., 2018). After a certain period of permanence in the atmosphere (up to 2 years, Schroeder and Munthe, 1998), Hg is deposited over terrestrial ecosystems through direct wet and dry precipitation and *via* litterfall. Because of its predominant atmospheric origin and its high affinity for the reduced sulphur groups of the organic matter, Hg tends to accumulate in the organic-matter rich superficial soil layers (i.e., 30–50 cm) (Skyllberg et al., 2006; Smith-Downey et al., 2010; Obrist et al., 2014; Obrist et al., 2017). For this reason, most of the Hg studies in terrestrial ecosystems are usually focused on the top few centimetres of soils (Xin and Gustin, 2007). However, on a minor scale, Hg can also occur in soils as a result of the weathering of soil parent material (Roulet et al., 1998; Guédron et al., 2006; Peña-Rodríguez et al., 2014; Kroonenberg et al., 2022). As a consequence, Hg derived from lithological sources could be also contributing significantly to the total Hg soil pool, especially in the deepest soil horizons (Fiorentino et al., 2011; Richardson et al., 2018; Kroonenberg et al., 2022). The participation of the deep soil layers in Hg storage would strengthen the role of soils as a main reservoir of atmospheric Hg in terrestrial ecosystems, as well as making it less probable that Hg would reach aquatic ecosystems (Amos et al., 2013). Unfortunately, few recent studies have explored the relevance of soil deep horizons in the biogeochemical fate of Hg in soil, as most of them were restricted to the surface soil horizons (Richardson et al., 2018; Schuster et al., 2018; Kroonenberg et al., 2022; Richardson, 2022; Richardson, 2022). In the deepest soils layers, soil components other than C, such as Al and Fe oxyhydroxides or organic Al and Fe compounds, have been recognized to influence the vertical pattern of Hg in soils (Do Valle et al., 2005; Guédron et al., 2006; Navrátil et al., 2014; Richardson et al., 2018; Gómez-Armesto et al., 2020).

Podzols and soils with podzolic characteristics can serve as examples of soils with a recognized ability to accumulate Hg in the deeper soil horizons. In Podzols, Hg can be mobilized through the soil profile together with organic matter and Al and Fe compounds and afterwards immobilized due to its adsorption to metal (Al, Fe)-humus complexes and Al and Fe oxyhydroxides, leading to the characteristic soil vertical pattern of Hg reported in different works (Guédron et al., 2009; Navrátil et al., 2014; Richardson et al., 2018; Gómez-Armesto et al., 2020; Gómez-Armesto et al., 2021a; Gómez-Armesto et al., 2021b).

Besides the particular chemical properties that determine Hg occurrence in soils such as Podzols, the distribution of Hg in other soils can also be defined by pedogenetic processes, past climate changes, or soil degradation processes (forest fires, deforestation, erosion) as reported by Obrist et al. (2018). In some cases, the soil can be removed whole or in part by climatic and/or erosive causes and deposited far away from its original area, whereas in other cases, surface soil layers are buried with soil mobilized through erosion. When this happens, it is quite probable that the appearance of polycyclic soils is a consequence of the action of several pedogenetic processes, as these soils show a complex mixture of chemical properties, soil compounds, and morphological features (Taboada-Castro et al., 1995; Peiteado Varela et al., 2002). In fact, a polycyclic soil is a soil developed under different climatic scenarios that led to different and, sometimes, contrasting pedogenetic processes, resulting in soil horizons that are not genetically related (Canarache et al., 2006). Thus, the multilingual dictionary of soil science supported by the Spanish Society of Soil Science (SECS-SLCS-IEC, 2023) indicates that the deeper part of a polycyclic soil derived from old pedogenetic processes may serve as parent material of the more recent and superficial part of the soil. The involvement of polycyclism processes, through the vertical arrangement of organic matter and Al and Fe oxyhydroxides along the soil profile, was reported to be responsible for vertical patterns of Hg in mountain forest soils from Tierra del Fuego, Argentina (Peña-Rodríguez et al., 2014). In summary, the substantial role of the pedogenetic processes in the soil Hg sequestration should be deciphered to assess the transcendence of soils in the biogeochemical cycle of Hg in terrestrial ecosystems.

The present study assess the occurrence, accumulation, and vertical distribution of Hg in three deep polycyclic soils from a mountain area in NW Iberia Peninsula. This study aims to evidence the relevance of deeper soil layers in terms of soil Hg pools, and attempts to further understand the main soil chemical characteristics and soil processes involved in the observed Hg patterns with soil depth.

MATERIAL AND METHODS

Study Area and Sampling Procedure

This study was carried out in the Xistral Mountains, a medium altitude mountain range (maximum 1,060 m a.s.l.) located in the north of the province of Lugo (Galicia). This area is characterized by a mean annual temperature between 7°C and 10°C, and a moderate total annual rainfall (1,400–1800 mm) with a scarce rainfall seasonality and abundant fogs throughout the year above 600 m a.s.l. (Pontevedra-Pombal et al., 2012). In the Xistral Mountains, three soil profiles developed from granitic materials and with a complex morphology were selected for the present study. These soils were denoted as FL (43° 31′42.8″ N, 7° 31′3.9″ W) MF (43° 28′6.7″ N, 7° 31′33.5″ W), and RV (43° 31′22.6″ N, 7° 29′54.9″ W), with a depth of 185, 190, and 155 cm, respectively. The vegetation in the three sampling sites was mostly dominated by different species of heather (*Erica* sp.), some individuals of shrubs species from genus *Ulex* and *Cytisus*, small patches of mosses (*Sphagnum* sp.), and several herbaceous species such as *Molinia caerulea* and *Agrostis curtisii*.

At each soil sampling site, samples were collected on a surface cut of a forest track, removing the first 30 cm-thickness of the profile in order to obtain a fresh soil surface and avoid potential anthropogenic disturbances. From each individual horizon

identified in the field, soil samples were collected at an interval of 10–20 cm with a plastic garden trowel, which was rinsed twice between samples with a diluted HNO_3 solution and then dried. The total number of soil samples collected was 45. In addition, a fresh rock sample representing the parent material for each sampled soil was collected. Soil and rock samples were stored in plastic bags and transported to the laboratory in a portable fridge at 4°C. Once in the laboratory, after plant debris and stone removal, soil samples were air-dried and sieved (2-mm mesh), whereas rock samples were washed with distilled water and any soil residue removed. Approximately 0.5 kg of sieved soil was quartered with a stainless steel riffle-splitter to obtain samples with enough representativeness and homogeneity for subsequent general chemical characterization and Hg analyses.

Analytical Methods

The physico-chemical characterization of soil samples was carried out in the fine earth fraction (<2 mm). Soil pH was determined in soil suspensions obtained after addition of distilled water (pH_w) or saline solution (0.1 M KCl, pH_K) to soil samples, maintaining a 1:2.5 soil:solution ratio. The total content of biophilic elements (i.e., C and N) were determined in an autoanalyzer after combustion of milled soil samples, with total C values assumed to be organic C due to the absence of inorganic carbonates in the studied soils. Neutral saline solutions, 1 M NH_4Cl (Peech et al., 1947) and 1 M KCl (Al_K; Lin and Coleman, 1960) were used to displace exchangeable base cations (K_e, Na_e, Ca_e, Mg_e) and exchangeable Al. The sum of all displaced exchangeable cations was considered an estimate of the effective cation exchange capacity (eCEC). Soil texture was obtained on the basis of the particle-size distribution, which was determined after wet sieving (sand fractions) and the pipette method based in the sedimentation rate of soil particles for silt and clay fractions (Gee and Bauder, 1986).

The fractionation of Al and Fe in soil samples was carried out following the procedures used by García-Rodeja et al. (2004). Aluminium and Fe complexed by soil organic matter were obtained after extraction with 0.1 M Na-pyrophosphate solution (Al_p, Fe_p). A 0.2 M ammonium oxalate-oxalic acid solution buffered at pH 3 was used to dissolve all non-crystalline Al and Fe compounds (Al_o, Fe_o) including poorly-ordered inorganic Al and Fe oxyhydroxides and metal (Al, Fe)-humus complexes. To estimate the total free pools, a 0.5 M NaOH solution was used in the case of Al (Al_n) while an Na-dithionite-citrate solution was applied for Fe (Fe_d). After these extractions, the following fractions of Al and Fe were operatively defined: a) metal (Al, Fe)-humus complexes which are equal to Al_p and Fe_p; b) inorganic non-crystalline Al and Fe compounds (Al_{ia}, Fe_{ia}) as the subtraction among the amounts of Al and Fe extracted with oxalate-oxalic acid and Na-pyrophosphate; c) crystalline Al and Fe compounds (Al_c, Fe_c) from the result of total free Al and Fe minus oxalate-oxalic acid extractable Al and Fe. To extend the characterization of the organically complexed Al pool, two additional extractions were carried out using two chloride salt solutions, namely, 0.5 M $CuCl_2$ (Juo and Kamprath, 1979) and 0.33 M $LaCl_3$ (Bloom et al., 1979), denoted as Al_{Cu} and Al_{La}, respectively. Following previous studies (Urrutia et al., 1995; García-Rodeja et al., 2004), chloride salt solutions provide the operative differentiation of Al-humus complexes in the following types: high stability Al-humus complexes (Al_{oh}, as Al_p–Al_{Cu}), moderate stability (Al_{om}, as Al_{Cu}–Al_{La}) and low stability (Al_{ol}, Al_{La}–Al_K). The concentration of Al and Fe in the different extractions was determined by flame-AAS spectrometry. Carbon solubilized during the Na-pyrophosphate extract (C_p) was determined by titration with 0.1 N Mohr salt and considered an estimation of well humified soil organic matter.

For the Hg measurement, samples of soil and rock were milled in a mechanical agate mortar (Retsch RM100, Retsch RM200). About 100 mg of each sample was analyzed twice using a DMA-80 Hg analyzer (Milestone), which is based on thermal decomposition and atomic absorption spectroscopy. Measurements were repeated when the coefficient of variation was higher than 10%. In order to test the accuracy of the method (for quality assurance and quality control purposes), different standard reference materials were analyzed at the start of each sample run and every fifteen samples, obtaining recovery percentages of 91% for GBW 07402 (average 13.6 ± 0.7 μg kg^{-1}; n = 12) and 91% for GBW 07427 (average 47.4 ± 9.8 μg kg^{-1}; n = 9). Finally, the detection limit of the method was 0.043 μg kg^{-1}.

Mercury Reservoir Evaluation

For each sampled depth, the pool of Hg (Hg_{Res_d}) was calculated taking into account the corresponding thickness (T_d), bulk density (B_d), coarse fragment proportion (C) (%), and total Hg content (HgT) as in Wang et al. (2017).

$$Hg_{Res\_d} = Hg_T \, x \, B_d \, x \, T_d \, x \, (1 - C)$$

The Hg reservoir in each soil horizon identified (Hg_{Tres}) was calculated as the sum of all Hg_{Res_d} included in the same horizon.

Relative Hg Losses and Gains During Weathering

Mass transfer coefficients of Hg (τ_{Hg}) were calculated following the open-system mass transport function (Guédron et al., 2006; Fiorentino et al., 2011; Guédron et al., 2013; Richardson, 2022; Spinola et al., 2022) for each sample depth, in order to evaluate Hg depletions or enrichments and to discriminate among possible sources of Hg (atmospheric deposition or lithogenic origin) in the soil profiles. The chosen immobile element for calculations was zirconium and its concentrations in soil (*subscript s*) and parent material (*subscript r*) of both elements (Hg as mobile element and Zr as immobile element) were used as follows:

$$\tau_{Hg} = \frac{Hg_{T,s}}{Zr_{T,s}} * \frac{Zr_{T,r}}{Hg_{T,r}} - 1$$

The τ_{Hg} for each soil horizon identified was calculated as the average of all Tau values included in the corresponding depths analysed. As Spinola et al. (2022) indicated, positive τ values mean Hg enrichment of soil horizons regarding soil

TABLE 1 | Mean values per soil horizon of some chemical characteristics of FL, MF, and RV soils.

Profile	Horizon	Depth	[a]n	[b]pH_w	[b]pH_K	C	[c]C_p	N	S	[d]BS	[d]Al_K
		cm				---------- % ----------				$cmol_c\ kg^{-1}$	
FL	O	0–10	1	4.7	4.3	20.8	10.3	1.5	0.05	5.9	1.3
	A	10–30	2	4.8	3.9	11.3	7.1	0.7	0.05	1.3	6.5
	AC	30–50	2	5.1	4.1	5.0	4.3	0.3	0.02	0.3	4.3
	2A	50–60	1	4.8	4.2	5.7	5.1	0.3	0.01	0.3	3.7
	2AC	60–74	1	4.7	4.3	4.5	2.2	0.2	0.01	0.2	4.0
	2BC	74–90	1	4.7	4.4	3.2	2.9	0.1	0.01	0.2	1.9
	3BC	90–150	3	4.6	4.5	2.4	1.5	0.1	0.01	0.2	1.8
	3C	150–185	3	4.9	4.4	0.6	0.0	0.0	0.00	0.2	0.7
MF	A	0–38	3	4.8	3.6	10.9	5.9	0.6	0.03	1.6	5.2
	Bhs	38–48	1	5.0	4.3	3.0	1.7	0.1	0.01	0.2	2.1
	Bs	48–68	1	5.0	4.4	3.9	3.2	0.2	0.01	0.3	2.1
	2CB	68–100	2	5.1	4.5	1.6	1.0	0.1	0.00	0.2	1.3
	3C	100–190	6	5.2	4.3	0.6	0.1	0.0	0.00	0.4	1.2
RV	A	0–43	4	4.8	4.2	7.7	5.7	0.5	0.03	0.6	4.2
	B	43–75	6	4.8	4.5	4.5	3.9	0.3	0.02	0.4	1.8
	2A	75–95	3	4.7	4.4	3.1	2.2	0.2	0.01	0.4	1.7
	2AB	95–110	2	4.7	4.5	1.2	0.9	0.1	0.01	0.4	1.1
	2B	110–140	2	4.8	4.3	0.3	0.1	0.0	0.01	0.4	1.5
	2C	140–155	1	4.8	4.0	0.1	0.0	0.0	0.01	0.3	1.8

[a]*n is the number of samples for each soil horizon.*
[b]*pH_w and pH_K are soil pH in water and in saline solution.*
[c]*C_p is the pyrophosphate-extracted C.*
[d]*BS is the sum of base cations (Ca, Mg, Na, K) and Al_K is the exchangeable Al.*

parent material, negative τ values signal Hg losses, and if zero values are obtained Hg is stable in the horizon in relation to the parent material or there is net gain/loss of Hg in that horizon.

Statistical Treatment of Data and Calculations

All the statistical analyses described in this section were done using SPSS version 25.0 software for Windows.

In order to reduce the number of soil variables studied into a few components, a principal component analysis (PCA) was conducted, applying varimax rotation that maximizes the sum of the variances of the square loadings. Each principal component consisted of variables with loadings higher than 0.50 (Abdi and Williams, 2010).

A principal component regression (PCR) analysis was carried out with the "new" variables obtained in the PCA as independent variables, and the principal components which are not correlated between them (orthogonal) and Hg as dependent variables. Using this method, we could predict Hg concentration and distinguish which soil properties are most involved in the Hg depth distribution observed. The weight of each component (wPC) was used to calculate its participation in the Hg prediction and it was estimated by multiplying the score of each component by the corresponding standardized regression coefficient (Liu et al., 2003). The accuracy of the model was checked through root mean squared error (RMSE) calculation and through the representation of Hg observed vs. predicted.

RESULTS AND DISCUSSION

Main Characteristics of Soils

The general chemical properties of the three soil profiles are shown in **Table 1** as an average per soil horizon type. The pH in distilled water (pH_w) ranged from 4.6 to 5.2, and in saline solution (pH_K) was about 0.2–1.1 units lower than pH_w. The range of pHw is quite similar to that reported in previous studies on forest soils derived from granitic material, varying from 4.5 to 5.3 (Álvarez et al., 2002; Eimil-Fraga et al., 2015). The strong acidity showed by the studied soils, which was more evident in the A horizons, is expected considering the low content of weatherable minerals in the soil parent material as well as the climatic conditions that favour the loss of base cations through leaching (Macías et al., 1982). In addition, the contribution of the exchangeable acidity associated with proton release from organic matter functional groups and Al-humus complexes can also contribute to the observed acidity, as was evidenced in highly complex colluvial soils (Kaal et al., 2008) and in podzolic soils (Ferro-Vázquez et al., 2014). Since there are no carbonates in these soils, the total carbon is assumed to be equal to organic C and it ranged from 20.8% in organic horizons to 0.1% in the deepest C soil horizons. The highest Na-pyrophosphate extracted C (C_p)/C ratios occurred in the buried A horizons as well as in the illuvial horizons of MF, indicating the presence of well-humified and reactive organic matter in them which may be mobilized as metal-humus complexes (Ferro-Vázquez et al., 2014). As expected, due to the strong acidity of the studied soils, the sum of the base cations was very low in all horizons (0.2–5.9 $cmol_c\ kg^{-1}$), while the exchangeable Al (Al_K) was slightly high

TABLE 2 | Mean contents per soil horizon of Al and Fe compounds and Hg (Hg_T), total reservoir of Hg ($\sum Hg_{Tres}$) and Tau.

Profile	Horizon	Depth	[a]n	[b]Al_p	[b]Al_o	[b]Al_n	[b]Fe_p	[b]Fe_o	[b]Fe_d	[c]Hg_T	[c]$\sum Hg_{Tres}$	[d]τ_{Hg}
		cm		g kg^{-1}						μg kg^{-1}	mg m^{-2}	
FL	O	0–10	1	4.7	4.8	5.2	4.9	5.8	7.1	169	8.6	460.4
	A	10–30	2	4.4	4.7	5.8	4.7	6.5	6.9	117	20.2	199.0
	AC	30–50	2	4.6	5.5	5.7	4.9	4.9	6.3	44	7.0	72.5
	2A	50–60	1	8.6	10.0	10.7	7.1	9.0	9.9	79	6.6	135.3
	2AC	60–74	1	8.9	9.8	12.8	5.3	6.4	7.3	91	10.0	137.3
	2BC	74–90	1	6.8	9.9	10.6	2.4	2.5	3.8	47	7.0	83.4
	3BC	90–150	3	6.3	9.3	16.2	1.2	1.7	1.7	36	22.6	58.2
	3C	150–185	3	2.2	3.0	17.5	0.6	0.8	2.7	15	5.7	20.4
MF	A	0–38	3	4.4	5.2	5.9	4.8	7.1	8.8	139	29.3	59.4
	Bhs	38–48	1	6.7	7.7	10.2	4.6	8.1	9.4	52	3.5	44.6
	Bs	48–68	1	11.3	13.3	18.9	2.8	3.7	6.8	93	11.3	23.3
	2CB	68–100	2	4.7	9.0	9.3	1.6	2.2	4.8	40	9.9	13.7
	3C	100–190	6	2.1	4.1	18.3	1.5	1.9	6.0	22	12.5	9.4
RV	A	0–43	4	9.4	10.0	11.9	7.3	7.5	12.5	113	29.0	3.2
	B	43–75	6	9.0	15.0	16.2	7.2	8.6	14.2	129	32.5	5.0
	2A	75–95	3	5.7	10.0	14.8	3.4	3.9	7.5	88	13.3	2.3
	2AB	95–110	2	2.7	5.7	13.7	1.2	1.6	4.0	28	3.0	0.4
	2B	110–140	2	1.3	2.8	16.7	0.8	1.2	3.1	15	4.1	–0.5
	2C	140–155	1	0.7	1.4	17.5	0.4	0.6	2.7	9	1.5	–0.6

[a]*n is the number of samples for each soil horizon.*

[b]*Al_p (Fe_p), Al_o (Fe_o), Al_n and Fe_d are Al (Fe) extracted with Na-pyrophosphate (p), ammonium oxalate-oxalic acid (o), Al extracted with Na hydroxide (n) and Fe extracted with Na-dithionite-citrate (d), respectively.*

[c]*Hg_T and Hg_{Tres} are total mercury content and the mass of total Hg in areal basis for each whole horizon.*

[d]*τ_{Hg} are the mass transfer coefficients of Hg for each whole horizon.*

(0.7–6.5 $cmol_c$ kg^{-1}), especially in the surface and buried A horizons, where it dominated the cation exchange capacity of the soils. Both the exchangeable base cations and exchangeable Al are in the range of values reported for acid forest soils developed from parent materials poor in weatherable minerals such as granite, micaceous schist, slates, or quartzites (Álvarez et al., 2002; Eimil-Fraga et al., 2015; Cutillas-Barreiro et al., 2016). Unless in the case of the O layer of FL soil, Al dominated the cation exchange complex in the studied soils (range 0.7–6.5 $cmol_c$ kg^{-1}) which is characteristic in acid forest soils.

The distribution of the Al and Fe compounds in the soil solid phase of the different horizons studied is summarized in **Table 2**. The Al distribution is dominated by the non-crystalline compounds (Al_o) in the O, A, and B horizons ranging from 4.7 to 15.0 g kg^{-1}, although in most of the cases Al-hummus complexes (Al_p) represented more than 60% of total non-crystalline Al compounds. The predominance of non-crystalline Al compounds is often reported in mountain acid forest soils from NW Iberian Peninsula (García-Rodeja and Macías, 1986; Álvarez et al., 2002). On the other hand, Al_c (secondary crystalline Al compounds, estimated as the difference of Al_n minus Al_o) showed a notable predominance in the deepest soil layers (mostly C or transitional B/C horizons) representing 42%–92% of the total free Al pool. A greater abundance of crystalline compounds, compared to other non-ordered Al compounds, was shown by García-Rodeja and Macías (1986) in low organic C content horizons of soils derived from weathered granitic materials located in mountain areas. With regard to organically-complexed Al compounds, its distribution is dominated by Al-humus complexes of moderate (Al_{om}) and high stability (Al_{oh}) below 20–30 cm depth in the three soil profiles, showing values in ranges of 4–37 and 4–91 $cmol_c$ kg^{-1}, respectively. These values are in the same order as those reported in previous studies where Al fractionation in acid forests soils was assessed (Álvarez et al., 2002; Kaal et al., 2008; Ferro-Vázquez et al., 2014), and combined, Al_{om} and Al_{oh} accounted for 51%–99% of the total Al-humus complexes (**Figure 1**). Consistently with Eimil-Fraga et al. (2015), the degree of organic matter humification in the FL, MF, and RV soils, indirectly assessed through the C/N ratio, would favour the organic matter-Al interactions and the consequent formation of high stability Al-humus complexes.

In the case of the Fe distribution, organically-complexed Fe (Fe_p) dominate in the A horizons (4.7–7.3 g kg^{-1}), whereas in the B and C horizons there is an equal partition between Fe-hummus complexes (Fe_p) and crystalline compounds (Fe_c) (**Table 2**). The range of Fe values extracted with different solutions (0.4–14.2 g kg^{-1}) is quite similar to that reported by Kaal et al. (2008) for soils with a noticeable polycyclic pedogenetic character. The trend observed in the fractionation of Fe in FL, MF, and RV coincides with that reported for acid soils from mountain areas (Ferro-Vázquez et al., 2014; Gómez-Armesto et al., 2021a).

Considering the morphological features observed during field sampling such as the horizon diversity and discontinuities recognisable by the occurrence of stone lines and charcoal and the previous discussion of main soil physicochemical characteristics, the three soils studied are representative of complex polycyclic soils typically found in the mountain landscapes from NW Iberian Peninsula. According to this and

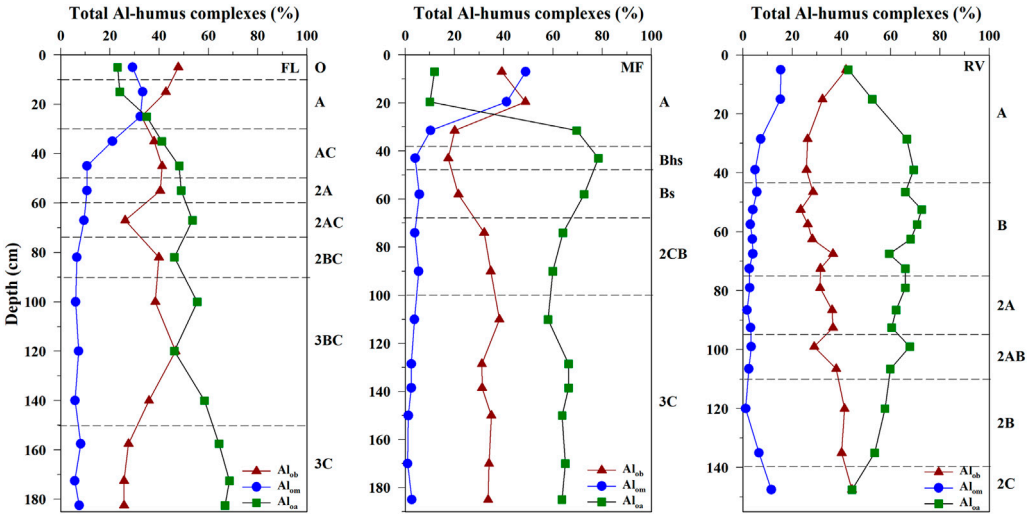

FIGURE 1 | Vertical patterns of Al-humus complexes of low (Al_{ob}), moderate (Al_{om}) and high stability (Al_{oa}) in the soils FL, MF, and RV.

following the IUSS-WRB (2014), although some classification requirements could be not wholly satisfied such as colour in the illuvial horizons, a tentative classification of the studied soil was Folic Umbrisol for soils FL and MF and Cambic Umbrisol in the case of RV soil.

Total Mercury Content and Pools

The total mercury content (Hg_T) is shown in **Table 2** as an average per type of horizon. In general, the highest Hg concentrations are found in the organic matter rich horizons of the three soils (O and A) as well as in illuvial horizons, whereas the minimum Hg_T is observed in the C horizons of the studied soil profiles. Values of Hg_T in the uppermost soils layers of the three soils were higher than the range 43–92 μg kg^{-1} estimated through deep neural network-regression kriging in topsoil samples (0–20 cm) from the NW Iberian Peninsula in a large-scale study carried out in the European Union (Ballabio et al., 2021). Greater values of Hg_T than expected in A and O horizons could be justified by, besides other factors, the altitude at which the studied soils were located, as according to previous research greater atmospheric Hg deposition is favoured in these areas (Blackwell and Driscoll, 2015; Wang et al., 2017). Indeed, in the abovementioned study of Ballabio et al. (2021), moderate Hg levels were found for the Cantabrian Mountains in whose western foothills are located the Xistral Mountains. Detailed revision of values of Hg_T in the studied soils reveals that maximum Hg_T in the FL profile was in the O horizon (169 μg kg^{-1}), diminishing steadily with the soil depth until the first buried soil appeared (horizons 2A and 2AC) where Hg ranges between 79 and 91 μg kg^{-1} (**Figure 2**; blue line). In the MF soil, the highest Hg content was observed in the surface A horizon (139 μg kg^{-1}) then decreasing in the Bhs horizons to increase again in the spodic Bs horizon (93 μg kg^{-1}). Contrary to the FL profile, the remains of older soil cycles in the MF site do not lead to subsurface peaks of Hg_T and this diminishes, progressively reaching the lowest values in the deepest horizon analysed (3C). As it can be seen in **Figure 2**, the maximum Hg_T in the RV soil does not occur in the uppermost soil layer (A horizon) but in the B horizon (129.2 μg kg^{-1}), although both horizons showed a relatively similar mean value. The buried soil in RV shows a noticeable Hg_T level in the 2A horizon (88 μg kg^{-1}), although somewhat lower than in the present soil cycle. Below the horizon 2A, Hg_T decreases with depth in the soil RV and the lowest value is observed in the deepest horizon with 9 μg kg^{-1}.

Although the Hg_T in the samples of the three soils studied were considerably higher than the values of Hg_T found in their parent material (0.7, 1.3, and 4.0 μg kg^{-1} for soils FL, MF and RV, respectively), most of the samples were below 130 μg kg^{-1}, the critical load of Hg in soils (Tipping et al., 2010). Previous studies have shown that in soils with background Hg levels, such as those from the present study, the proportion of available Hg scarcely reaches a percentage of 0.31% of Hg_T in acid soils (Frey and Rieder, 2013). Therefore, considering both the levels of Hg_T and the equivalent fraction of available Hg, the bacterial and fungal communities of the studied soils are not likely to be affected, as detrimental effects on these are only likely with values of Hg_T above 320 μg kg^{-1} (Frossard et al., 2017), almost twice that of the measured values. Moreover, only the surface horizons (O and A) and the B horizon of the soil RV have Hg concentrations somewhat higher than the natural background considered for non-polluted soils (<100 μg kg^{-1}; Xin and Gustin, 2007). This value of Hg_T (100 μg kg^{-1}) was also considered by Harris-Hellal et al. (2009) as a threshold below which no modifications were observed in the bacterial community structure. For plants and terrestrial invertebrates, toxicity effects were observed for Hg_T levels several orders of magnitude higher than those found in FL, MF, and RV soils (Mahbub et al., 2017).

In general, the values of Hg_T obtained in the present study are in the same order as those reported for acid forest soils not directly affected by Hg emission point sources worldwide (Du et al., 2019; Gruba et al., 2019; Nave et al., 2019; Gómez-Armesto et al., 2021a, 2021b; Kroonenberg et al., 2022). Beyond the values

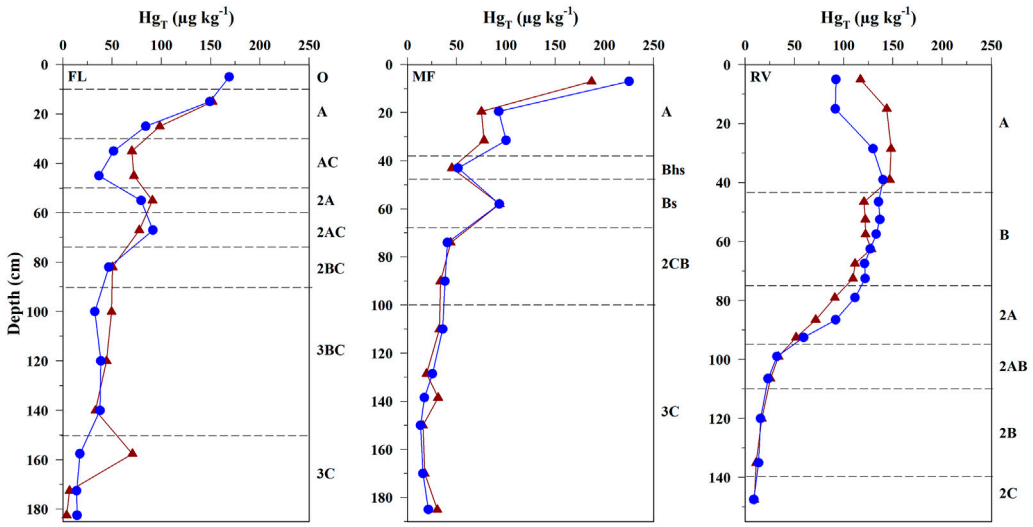

FIGURE 2 | Variation of observed (blue circles) vs. predicted Hg (red triangles) with soil depth in the soils FL, MF, and RV.

of Hg_T, the variation of Hg concentrations with soil depth should also be considered. The progressive diminution of Hg_T values with soil depth observed in the three studied soils, besides the very low values of Hg in the parent material, indicates a predominance of atmospheric against lithological Hg source, which reinforces atmospheric deposition as the main mechanism responsible for the occurrence of Hg in the soil surface. Previous studies that focused on the variation of Hg with soil depth also showed a noticeable diminution of Hg from the surface to bottom horizons (Fiorentino et al., 2011; Richardson et al., 2018; Gómez-Armesto et al., 2020; Kroonenberg et al., 2022; Richardson, 2022). However, as it can be seen from **Figure 2**, some parts of the soil profiles can depart from this general trend due to the effects of pedogenetic processes.

The Hg reservoir (Hg_{Tres}), shown in **Table 2**, was calculated as the sum of the absolute amount of Hg in each soil sample that compounds the horizon described for the studied soil profiles. The total Hg accumulated in the whole soil profile was 87.7, 66.5, and 83.4 mg m^{-2} for the FL, MF, and RV soils, respectively. On average, the studied soil profiles accumulated 79.2 mg m^{-2}, higher than the total Hg pool of the upper 40 cm of forest soils reported by Obrist et al. (2009) (from 4 to 7 mg m^{-2}), Zhou et al. (2017) (from 7.2 to 10.7 mg m^{-2}), and Obrist (2012) (from 3 to 40 mg m^{-2}). When evaluating the upper 60 cm of forest soils, Méndez López et al. (2023) assessed between 32 and 42 mg m^{-2} in the complete mineral soil profiles studied. Hg pools reported by Demers et al. (2007) (22 mg m^{-2} and 9.6 mg m^{-2} for deciduous and coniferous stands, respectively) are also lower than those reported in the almost 2-m-depth soil profiles of the current study. When comparing Hg pools from different studies, in addition to the uncertainties arising from their calculation for specific soil horizons and/or the complete soil profile (Zhou et al., 2020), different soil profiles depths should also be of concern. In fact, Hg_{Tres} reported for the upper meter of six different 10-m depth soil profiles by Richardson et al. (2018) were 26, 33, 48, 69, 98, and 246 mg Hg m^{-2}.

The Hg reservoir (8.6 mg m^{-2}) of the soil horizon with the highest Hg_T content (O horizon - FL soil profile) was higher than the range (0.02–7 mg m^{-2}) found for this type of horizon worldwide (Evans et al., 2005; Demers et al., 2007; Friedli et al., 2007; Obrist, 2012; Richardson et al., 2013 or Méndez López et al., 2023). The O layers are usually considered as the soil horizons more influenced by atmospheric Hg deposition, but despite this, higher Hg stocks were detected in singular horizons from these polycyclic soils like 2AC (FL soil), Bs and 3C (MF soil) or 2A (RV soil).

The horizons with the highest Hg_{Tres} were the B-horizon from RV soil (32.5 mg m^{-2}), located at 43–75 cm depth followed by both the surface A horizons from RV and MF soil profiles (29.0 and 29.3 mg m^{-2}, respectively). Similar thickness (32–41 cm depth), bulk density (0.81–0.99 g cm^{-3}) and high total Hg contents (113–139 µg kg^{-1}, **Table 2**) were responsible for similar Hg pools of these horizons. As an average, the Hg stored in the surface mineral horizons (A horizons upper 30 cm, ~26.2 mg m^{-2}) is comparable to that found by Richardson et al. (2018) in the upper 30 cm of several soils with values between 26 and 38 mg m^{-2}. At greater soil depths; Richardson et al. (2018) estimated higher Hg inventories as we observed in subsurface mineral horizons such as B from RV soil and the transition layer 3BC from FL soil. The Hg_{Tres} estimated for the 3BC layer (22.6 mg Hg m^{-2}) is mainly a consequence of its thickness (60 cm) and, to a lesser extent, to Hg_T content (36 µg kg^{-1}).

The lowest Hg_{Tres} occurred in the deepest sampled horizons from FL and RV soil profiles (3C: 5.7 mg Hg m^{-2} and 2C: 1.5 mg Hg m^{-2}, respectively) manly due to their low Hg_T contents and the Bhs horizon from MF soil (3.5 mg Hg m^{-2}) because of its low thickness (10 cm) and high coarse fragment proportion (54%). Therefore, the commonly observed declining pattern of Hg

concentrations with depth (Zhou et al., 2020) is broken when areal mass is taken into account because in addition to Hg concentrations, soil horizon properties related to soil genesis (density, coarse fraction content, horizon thickness, organic matter content, etc.) will influence the pattern distribution of Hg_{Tres}. As a result, deeper and subsurface soil horizons that are not commonly evaluated (>40–50 cm) because they are not suspicious for accumulating atmospheric Hg can evolve as true reservoirs with important environmental and health implications. The highest Hg pools observed in the deepest horizons (>40–50 cm) represented about 50%–65% of all the Hg stored in those soil profiles. This fact suggests that, if deep layers of soils are not evaluated, a big proportion of the Hg stored at a global level in soils will be systematically underestimated. Fluctuations in the pool of Hg observed with soil depth are even more prominent when looking at polycyclic soils due to the complex soil genesis involved. This has a great transcendence in environmental terms since Hg accumulated in deep soil horizons is associated with organic matter and Al and Fe compounds which are expected to contribute to the most recalcitrant soil Hg pools (Smith-Downey et al., 2010). In absence of anthropogenic perturbations such as forest fire or land-use changes, the biogeochemical stability of this soil Hg pool prevents its mobility to other components of terrestrial ecosystems, leaving aside toxicity risks to wildlife and human health as well as a decline in the quality of groundwater and surface waters.

The complexity of polycyclic soils is also conspicuous when evaluating possible gains and losses of Hg regarding parent material. The highest τ_{Hg} values in each soil profile (**Table 2**) were detected in current or older surface horizons (O, A and even AC horizons) showing that atmospheric deposition of Hg was, and still is, the main source of Hg in the soils evaluated. Moreover, regardless ofthose buried surface horizons, τ_{Hg} values decrease as soil profile depth increases and the lowest values were always calculated for the deepest horizons of each soil profile showing almost no influence of Hg from lithogenic sources. Close to zero τ_{Hg} negative values (−0.5 and −0.6 from 2B to 2C horizons from RV soil, respectively) were also interpreted as indicative of almost no atmospheric deposition. Compared to FL and MF soil horizons, τ_{Hg} values from RV soil are very low. They are comparable with those reported by different authors for a nearby active quarry soil profile in Brasil (Fiorentino et al., 2011), for different sites in a New York-Tennessee transect (Richardson, 2022), and for different forest soils in a nearby study area (Gómez Armesto et al., 2021). In all cases, τ_{Hg} values are mainly positive but less than 10. When focussing in FL and MF soil profiles, similar values of τ_{Hg} were only found in the deepest soil horizons. The soil FL is that with the highest τ_{Hg} values which are comparable to those found in soils nearby to gold mines (Guédron et al., 2006).

The mass transfer coefficients of Hg calculated for the three soil profiles were of different orders of magnitude but all indicated a net gain of Hg in the soil horizons regarding their parent material. In fact, the contribution from parent material to soil Hg accumulation is very low in almost all of the horizons evaluated. Taking into account that the studied polycyclic soils are located relatively close to one another and therefore climate conditions are assumed to be the same, in addition to exogenic inputs associated to atmospheric Hg deposition, pedogenetic processes should be also involved in Hg distribution accounting for its gains and losses throughout the soil profiles as it was indicated by Guédron et al. (2006).

Relationship Between Soil Properties and Hg Distribution

In order to understand the involvement of soil processes in Hg distribution through soil profiles, in addition to common soil properties derived from the general characterization of soil samples, the different forms of Fe and Al associated to the soil solid phase together with Hg concentrations were included in the PCA analysis. The PCA extracted four components (**Table 3**) that accounted for 87% of the variance. The soil properties included in each PC and their corresponding loadings are shown in **Table 3**. The highest variation of the data was explained by PC1 and PC2, which accounted for 36% and 30%, respectively. PC1 is mainly associated with soil organic matter, including variables such as C, N, or S, but

TABLE 3 | Loadings of the soil properties used in the principal component analysis.

	PC1	PC2	PC3	PC4	Com
N	**0.97**	0.18	0.09	0.01	0.98
C	**0.96**	0.21	0.14	−0.01	0.98
eCEC	**0.92**	0.01	0.33	−0.07	0.96
S	**0.91**	0.21	0.01	0.08	0.89
BS	**0.90**	−0.18	−0.15	−0.01	0.86
Al_K	**0.84**	0.07	0.45	−0.09	0.93
C_p	**0.83**	0.43	0.26	0.08	0.96
Al_{La}	**0.78**	0.22	0.53	−0.12	0.96
Al_{ol}	**0.74**	0.26	0.54	−0.13	0.93
pH_K	**−0.69**	0.33	−0.53	0.02	0.87
Al_o	−0.10	**0.93**	−0.19	0.11	0.93
Al_p	0.12	**0.93**	0.12	0.15	0.92
Al_{om}	0.15	**0.91**	0.11	−0.06	0.86
Al_{oh}	−0.09	**0.89**	−0.01	0.26	0.86
Al_{Cu}	0.47	**0.76**	0.32	−0.09	0.90
Al_c	−0.39	**−0.76**	−0.31	0.15	0.84
Fe_p	0.30	**0.72**	0.30	0.49	0.94
Fe_o	0.29	**0.70**	0.46	0.42	0.95
Fe_d	0.16	**0.63**	0.17	0.72	0.97
Alia	−0.35	**0.51**	−0.48	0.01	0.62
Feia	0.12	0.31	**0.70**	0.04	0.60
Al_n	−0.56	−0.07	**−0.57**	0.31	0.75
Fe_c	−0.10	0.29	−0.34	**0.84**	0.91
pH_w	−0.28	−0.45	0.08	**0.49**	0.53
Eigv	8.6	7.1	3.0	2.2	
Var	35.6	29.6	12.7	9.1	

PC1—PC4: components.
Com: communality, proportion of the variance of each parameter explained by the extracted components.
Eigv: eigenvalue.
Var: percentage of variance explained by each component.
Soil properties determining each principal component (PC) appear in bold.

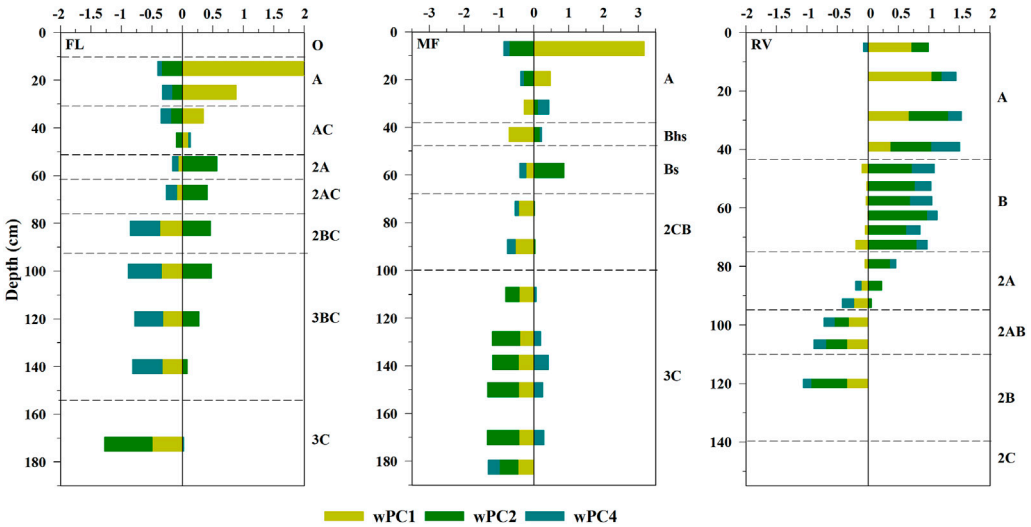

FIGURE 3 | Contribution of each principal component (wPC) to the predicted Hg_T of each sample (weight: regression standardized coefficient for a given component multiplied by the score).

also exchangeable cations and Al-hummus complexes of low stability. PC2 comprised reactive Al and Fe complexes, particularly those Al-hummus complexes of medium to high stability. PC3 explained 13% of the variance of the data and it was related to inorganic non-crystalline Fe compounds and total reactive Al with opposite sign. Finally, PC4 included crystalline Fe compounds and pH_w, accounting for 9% of the data variability.

In order to elucidate the influence of the soil properties in the Hg distribution observed in the three soil profiles studied, we performed a stepwise regression analysis using the scores of the four PCs extracted by PCA, considering them as new soil variables. The best model obtained included PC1, PC2, and PC4 with and adjusted R^2 of 0.893. The predicted Hg (Hg_{pred}) for each soil sample was estimated through the following Eq. **1**:

$$Hg_{pred} = 70.5 + 36.1^{*}PC1 + 28.9^{*}PC2 + 13.1^{*}PC4 \quad (1)$$

The model is rather accurate with a root mean-square error (RMSE) of 18 μg kg^{-1} for the whole group of samples as it can be seen in **Figure 2** in which we represented observed Hg_T values (blue circles) against predicted Hg (Hg_{pred}, red triangles). When focussing on how the principal soil components: PC1 (organic matter and low stability Al-hummus complexes), PC2 (reactive Al-Fe complexes and medium-high Al-hummus complexes), and PC4 (crystalline Fe compounds and pH_w) influence the depth Hg distribution of the studied soils (**Figure 3**), differences among the polycyclic soil horizons were observed. The main soil characteristics implied in the Hg_T distribution observed in A horizons are soil organic matter and low-stability Al-hummus complexes (PC1). In this sense, mercury is widely recognized to show a high affinity for the reduced sulphur groups of the organic matter (Khwaja et al., 2006; Skyllberg et al., 2006).

In the case of the FL soil, there is a clear effect of the PC2 (Al and Fe compounds), from the 2A horizon (50–60 cm) up to the 3C horizon in which, due to the low Hg values, no component showed influence. In the MF profile, of podzolic features, Al and Fe compounds, especially Al (Fe)-hummus complexes, showed the highest weights in Hg prediction. However, in the 3C horizon the crystalline Fe forms were the most important components in the estimation of the Hg content.

In the RV soil, the Hg content in the B and 2A horizons is mostly influenced by Al and Fe complexes (PC2) but also crystalline Fe (PC4) to a lesser extent. In this sense, secondary Fe minerals are recognized to promote Hg accumulation instead of organic compounds in those soil layers deeper than 1 m, as it was suggested by Richardson et al. (2018).

CONCLUSION

The results of this work indicated a noticeable contribution of the Hg deposition from the atmosphere to the Hg concentrations found in the soils studied instead of the lithological source. This fact is supported by the highest Hg values in surface horizons that diminished with depth and peaks in illuvial horizons which were, in all cases, considerably higher than the Hg concentrations of the parent material samples. The Hg depth distribution of the three soils studied was determined by the presence of soil components such as organic matter and Al and Fe complexes. Despite the fact that the maximum Hg contents were observed in O and A horizons, the highest Hg pools appeared in the deepest soil layers (>40–50 cm), representing about 50%–65% of all the Hg stored in those soil profiles. For this reason, subsurface soil horizons should be systematically evaluated in works about Hg

distribution in soils, since they could contribute substantially to the total Hg accumulated in soils worldwide. In addition, the biogeochemical stability of Hg accumulated in deep soil layers prevents its mobility to other components of terrestrial ecosystems, leaving aside toxicity risks to wildlife and human health as well as a decline in the quality of groundwater and surface waters.

DATA AVAILABILITY STATEMENT

The raw data supporting the conclusion of this article will be made available by the authors, without undue reservation.

AUTHOR CONTRIBUTIONS

All authors listed have made a substantial, direct, and intellectual contribution to the work and approved it for publication.

FUNDING

AG-A acknowledges to the Xunta de Galicia a predoctoral grant (ED481A-2016/220). MM-L acknowledges the predoctoral grant FPU of Ministerio de Educación y Formación Profesional (FPU17/05484). It is also recognized the financial support of the Consellería de Cultura, Educación e Universidade (Xunta de Galicia) through the contract ED431C2021/46-GRC granted to the research group BV1 of the University of Vigo and the research project ED431F2018/06-EXCELENCIA. The Spanish Ministry of Science and Innovation also supported this research through the funds provided to the project InMerForEcos (Ref. PID 2021-125114OB-I00).

CONFLICT OF INTEREST

The authors declare that the research was conducted in the absence of any commercial or financial relationships that could be construed as a potential conflict of interest.

REFERENCES

Abdi, H., and Williams, L. J. (2010). Principal Component Analysis. *Wiley Interdiscip. Rev. Comput. Stat.* 2, 433–459. doi:10.1002/wics.101

Álvarez, E., Monterroso, C., and Fernández Marcos, M. L. (2002). Aluminium Fractionation in Galician (NW Spain) Forest Soils as Related to Vegetation and Parent Material. *For. Ecol. Manag.* 166, 193–206. doi:10.1016/S0378-1127(01)00658-2

Amos, H. M., Jacob, D. J., Streets, D. G., and Sunderland, E. M. (2013). Legacy Impacts of All-Time Anthropogenic Emissions on the Global Mercury Cycle. *Glob. Biogeochem. Cycle* 27, 410–421. doi:10.1002/gbc.20040

Ballabio, C., Jiskra, M., Osterwalder, S., Borrelli, P., Montanarella, L., and Panagos, P. (2021). A Spatial Assessment of Mercury Content in the European Union Topsoil. *Sci. Total Environ.* 769, 144755. doi:10.1016/j.scitotenv.2020.144755

Blackwell, B. D., and Driscoll, C. T. (2015). Deposition of Mercury in Forests along a Montane Elevation Gradient. *Environ. Sci. Technol.* 49, 5363–5370. doi:10.1021/es505928w

Bloom, P. R., McBride, M. B., and Weaver, R. M. (1979). Aluminum Organic Matter in Acid Soils: Salt-Extractable Aluminum. *Soil Sci. Soc. Am. J.* 43, 813–815. doi:10.2136/sssaj1979.03615995004300040041x

Canarache, A., Vintila, I., and Munteanu, I. (2006). *Elsevier's Dictionary of Soil Science: Definitions in English with French, German, and Spanish Word Translations*. 1st. Amsterdam: Elsevier Science, 1354.

Clarkson, T. W., and Magos, L. (2006). The Toxicology of Mercury and its Chemical Compounds. *Crit. Rev. Toxicol.* 36 (8), 609–662. doi:10.1080/10408440600845619

Cutillas-Barreiro, L., Pérez-Rodríguez, P., Gómez-Armesto, A., Fernández-Sanjurjo, M. J., Álvarez-Rodríguez, E., Núñez-Delgado, A., et al. (2016). Lithological and Land-Use Based Assessment of Heavy Metal Pollution in Soils Surrounding a Cement Plant in SW Europe. *Sci. Total Environ.* 562, 179–190. doi:10.1016/j.scitotenv.2016.03.198

Demers, J. D., Driscoll, C. T., Fahey, T. J., and Yavitt, J. B. (2007). Mercury Cycling in Litter and Soil in Different Forest Types in the Adirondack Region, New York, USA, *Ecol. Appl.* 17-5, 1341–1351. doi:10.1890/06-1697.1

Do Valle, C. M., Santana, G. P., Augusti, R., Egreja-Filho, F. B., and Windmöller, C. C. (2005). Speciation and Quantification of Mercury in Oxisol, Ultisol, and Spodosol from Amazon (Manaus, Brazil). *Chemosphere* 58, 779–792. doi:10.1016/j.chemosphere.2004.09.005

Driscoll, C. T., Mason, R. P., Chan, H. M., Jacob, D. J., and Pirrone, N. (2013). Mercury as a Global Pollutant: Sources, Pathways, and Effects. *Environ. Sci. Technol.* 47, 4967–4983. doi:10.1021/es305071v

Du, B., Zhou, J., Zhou, L., Fan, X., and Zhou, J. (2019). Mercury Distribution in the Foliage and Soil Profiles of a Subtropical Forest: Process for Mercury Retention in Soils. *J. Geochem. Explor.* 205, 106337. doi:10.1016/j.gexplo.2019.106337

Eimil-Fraga, C., Álvarez-Rodríguez, E., Rodríguez-Soalleiro, R., and Fernández-Sanjurjo, M. J. (2015). Influence of Parent Material on the Aluminium Fractions in Acidic Soils under *Pinus pinaster* in Galicia (NW Spain). *Geoderma* 255-256, 50–57. doi:10.1016/j.geoderma.2015.04.026

Evans, G., Norton, S. A., Fernandez, I. J., Kahl, J. S., and Hanson, D. (2005). Changes in Concentrations of Major Elements and Trace Metals in Northeastern U.S.-Canadian Sub-alpine Forest Floors. *Water Air Soil Pollut.* 163, 245–267. doi:10.1007/s11270-005-0435-2

Ferro-Vázquez, C., Nóvoa-Muñoz, J. C., Costa-Casais, M., Klaminder, J., and Martínez-Cortizas, A. (2014). Metal and Organic Matter Immobilization in Temperate Podzols: A High Resolution Study. *Geoderma* 217-218, 225–234. doi:10.1016/j.geoderma.2013.10.006

Fiorentino, J. C., Enzweiler, J., and Angélica, R. S. (2011). Geochemistry of Mercury along a Soil Profile Compared to Other Elements and to the Parental Rock: Evidence of External Input. *Water Air Soil Pollut.* 221, 63–75. doi:10.1007/s11270-011-0769-x

Frey, B., and Rieder, S. R. (2013). Response of Forest Soil Bacterial Communities to Mercury Chloride Application. *Soil Biol. Biochem.* 65, 329–337. doi:10.1016/j.soilbio.2013.06.001

Friedli, H. R., Radke, L. F., Payne, N. J., McRae, D. J., Lynham, T. J., and Blake, T. W. (2007). Mercury in Vegetation and Organic Soil at an Upland Boreal Forest Site in Prince Albert National Park, Saskatchewan, Canada. *J. Geophys. Res.* 112, G01004. doi:10.1029/2005JG000061

Frossard, A., Hartmann, M., and Frey, B. (2017). Tolerance of the Forest Soil Microbiome to Increasing Mercury Concentrations. *Soil Biol. Biochem.* 105, 162–176. doi:10.1016/j.soilbio.2016.11.016

García-Rodeja, E., Nóvoa, J. C., Pontevedra, X., Martínez-Cortizas, A., and Buurman, P. (2004). Aluminium Fractionation of European Volcanic Soils by Selective Dissolution Techniques. *Catena* 56, 155–183. doi:10.1016/j.catena.2003.10.009

García-Rodeja, E., and Macías, F. (1986). Aplicación de técnicas de disolución selectiva al estudio de componentes no cristalinos de una secuencia de suelos sobre granito en la sierra de Ancares (Lugo, Galicia). *An. Edaf. Agrob.* 45, 347–366.

Gee, G. W., and Bauder, J. W. (1986). "Particle Size Analysis," in *Methods of Soil Analysis. Part A*. Editor A. Klute (Madison: American Society of Agronomy), 383–411.

Gómez-Armesto, A., Martínez-Cortizas, A., Ferro-Vázquez, C., Méndez-López, M., Arias-Estévez, M., and Nóvoa-Muñoz, J. C. (2020). Modelling Hg Mobility

in Podzols: Role of Soil Components and Environmental Implications. *Environ. Pollut.* 260, 114040. doi:10.1016/j.envpol.2020.114040

Gómez-Armesto, A., Méndez-López, M., Pontevedra-Pombal, X., García-Rodeja, X., Alonso-Vega, F., Arias-Estévez, M., et al. (2021a). Soil Properties Influencing Hg Vertical Pattern in Temperate Forest Podzols. *Environ. Res.* 193, 110552. doi:10.1016/j.envres.2020.110552

Gómez-Armesto, A., Méndez-López, M., Marques, P., Pontevedra-Pombal, X., Monteiro, F., Madeira, M., et al. (2021b). Patterning Total Mercury Distribution in Coastal Podzolic Soils from an Atlantic Area: Influence of Pedogenetic Processes and Soil Components. *Catena* 206, 105540. doi:10.1016/j.catena.2021.105540

Gruba, P., Socha, J., Pietrzykowski, M., and Pasichnyk, D. (2019). Tree Species Affects the Concentration of Total Mercury (Hg) in Forest Soils: Evidence from a Forest Soil Inventory in Poland. *Sci. Total. Environ.* 647, 141–148. doi:10.1016/j.scitotenv.2018.07.452

Guédron, S., Grangeon, S., Jouravel, G., Charlet, L., and Sarret, G. (2013). Atmospheric Mercury Incorporation in Soils of an Area Impacted by a Chlor-Alkali Plant (Grenoble, France): Contribution of Canopy Uptake. *Sci. Total Environ.* 445-446, 356–364. doi:10.1016/j.scitotenv.2012.12.084

Guédron, S., Grangeon, S., Lanson, B., and Grimaldi, M. (2009). Mercury Speciation in a Tropical Soil Association; Consequence of Gold Mining on Hg Distribution in French Guiana. *Geoderma* 153, 331–346. doi:10.1016/j.geoderma.2009.08.017

Guédron, S., Grimaldi, C., Chauvel, C., Spadini, L., and Grimaldi, M. (2006). Weathering versus Atmospheric Contributions to Mercury Concentrations in French Guiana Soils. *Appl. Geochem.* 21, 2010–2022. doi:10.1016/j.apgeochem.2006.08.011

Harris-Hellal, J., Vallaeys, T., Garnier-Zarli, E., and Bousserrhine, N. (2009). Effects of Mercury on Soil Microbial Communities in Tropical Soils of French Guyana. *Appl. Soil Ecol.* 41, 59–68. doi:10.1016/j.apsoil.2008.08.009

IUSS Working Group WRB (2014). International Soil Classification System for Naming Soils and Creating Legends for Soil Maps. World Reference Base for Soil Resources 2014. World Soil Resources Reports No. 106. Rome: FAO, 181.

Juo, A. S. R., and Kamprath, E. J. (1979). Copper Chloride as an Extractant for Estimating the Potentially Reactive Aluminum Pool in Acid Soils. *Soil Sci. Soc. Am. J.* 43, 35–38. doi:10.2136/sssaj1979.03615995004300010006x

Kaal, J., Costa-Casais, M., Ferro-Vázquez, C., Pontevedra-Pombal, X., and Martínez-Cortizas, A. (2008). Soil Formation of "Atlantic Rankers" from NW Spain-A High Resolution Aluminium and Iron Fractionation Study. *Pedosphere* 18, 441–453. doi:10.1016/S1002-0160(08)60035-1

Khwaja, A. R., Bloom, P. R., and Brezonik, P. L. (2006). Binding Constants of Divalent Mercury (Hg^{2+}) in Soil Humic Acids and Soil Organic Matter. *Environ. Sci. Technol.* 40, 844–849. doi:10.1021/es051085c

Kroonenberg, S., Wong, T., Bijnaar, G., Finkie, R., Goenopawiro, K., Asneel, S., et al. (2022). Mercury Background Values in Soils and Saprolites in the Gold-Rich Greenstone Belt of Suriname, Guiana Shield: The Role of Parent Rock and Residual Enrichment. *Sci. Total Environ.* 848, 157631. doi:10.1016/j.scitotenv.2022.157631

Lin, C., and Coleman, N. T. (1960). The Measurement of Exchangeable Aluminum in Soils and Clays. *Soil Sci. Soc. Am. J.* 24, 444–446. doi:10.2136/sssaj1960.03615995002400060009x

Liu, R. X., Kuang, J., Gong, Q., and Hou, X. L. (2003). Principal Component Regression Analysis with SPSS. *Comput. Methods Progr. Biomed.* 71, 141–147. doi:10.1016/S0169-2607(02)00058-5

Macías, F., Calvo, R., García-Rodeja, E., García, C., and Silva, B. (1982). El material original: su formación e influencia en las propiedades de los suelos de Galicia. *An. Edafol. Agrobiol.* 47: 1747–1768.

Mahbub, K. R., Krishnan, K., Naidu, R., Andrews, S., and Megharaj, M. (2017). Mercury Toxicity to Terrestrial Biota. *Ecol. Indic.* 74, 451–462. doi:10.1016/j.ecolind.2016.12.004

Méndez-López, M., Parente-Sendín, A., Calvo-Portela, N., Gómez-Armesto, A., Eimil-Fraga, C., Alonso-Vega, F., et al. (2023). Mercury in a Birch Forest in SW Europe: Deposition Flux by Litterfall and Pools in Aboveground Tree Biomass and Soils. *Sci. Total Environ.* 856, 158937. doi:10.1016/j.scitotenv.2022.158937

Nave, L. E., Covarrubias Ornelas, A., Drevnick, P. E., Gallo, A., Hatten, J. A., Heckman, K. A., et al. (2019). Carbon–mercury Interactions in Spodosols Assessed through Density Fractionation, Radiocarbon Analysis, and Soil Survey Information. *Soil Sci. Soc. Am. J.* 83, 190–202. doi:10.2136/sssaj2018.06.0227

Navrátil, T., Shanley, J., Rohovec, J., Hojdová, M., Penížek, V., and Buchtová, J. (2014). Distribution and Pools of Mercury in Czech Forest Soils. *Water Air Soil Pollut.* 225, 1829. doi:10.1007/s11270-013-1829-1

Obrist, D., Agnan, Y., Jiskra, M., Olson, C. L., Colegrove, D. P., Hueber, J., et al. (2017). Tundra Uptake of Atmospheric Elemental Mercury Drives Arctic Mercury Pollution. *Nature* 547, 201–204. doi:10.1038/nature22997

Obrist, D., Johnson, D. W., and Lindberg, S. E. (2009). Mercury Concentrations and Pools in Four Sierra Nevada Forest Sites, and Relationships to Organic Carbon and Nitrogen. *Biogeosciences* 6, 765–777. doi:10.5194/bg-6-765-2009

Obrist, D., Kirk, J. L., Zhang, L., Sunderland, E. M., Jiskra, M., and Selin, N. E. (2018). A Review of Global Environmental Mercury Processes in Response to Human and Natural Perturbations: Changes of Emissions, Climate, and Land Use. *Ambio* 47, 116–140. doi:10.1007/s13280-017-1004-9

Obrist, D. (2012). Mercury Distribution across 14 U.S. Forests. Part II: Patterns of Methyl Mercury Concentrations and Areal Mass of Total and Methyl Mercury. *Environ. Sci. Technol.* 46, 5921–5930. doi:10.1021/es2045579

Obrist, D., Pokharel, A. K., and Moore, C. (2014). Vertical Profile Measurements of Soil Air Suggest Immobilization of Gaseous Elemental Mercury in Mineral Soil. *Environ. Sci. Technol.* 48, 2242–2252. doi:10.1021/es4048297

Peech, M., Alexander, L. T., Dean, L. A., and Fielding Reed, J. (1947). *Methods of Soil Analysis for Soil-Fertility Investigations*. U.S. Dept. of Agriculture. Washington DC, 757.

Peiteado Varela, E., Piñeiro Rebolo, R., and Martínez Cortizas, A. (2002). Distribución de algunos elementos mayores (K, Ca, Ti,Fe) y traza (Ga, Rb, Sr, Y, Zr, Br) en dos suelos policíclicos podsólicos. *Edafología* 9, 61–84.

Peña-Rodríguez, S., Pontevedra-Pombal, X., Gayoso, E. G. R., Moretto, A., Mansilla, R., Cutillas-Barreiro, L., et al. (2014). Mercury distribution in a toposequence of sub-Antarctic forest soils of Tierra del Fuego (Argentina) as consequence of the prevailing soil processes. *Geoderma* 232-234, 130–140. doi:10.1016/j.geoderma.2014.04.040

Pontevedra-Pombal, X., Rey-Salgueiro, L., García-Falcón, M. S., Martínez-Carballo, E., Simal-Gándara, S., and Martíez-Cortizas, A. (2012). Pre-industrial Accumulation of Anthropogenic Polycyclic Aromatic Hydrocarbons Found in a Blanket Bog of the Iberian Peninsula. *Environ. Res.* 116, 36–43. doi:10.1016/j.envres.2012.04.015

Richardson, J. B., Aguirre, A. A., Buss, H. L., Toby O'Geen, A., Gu, X., Rempe, D. M., et al. (2018). Mercury Sourcing and Sequestration in Weathering Profiles at Six Critical Zone Observatories. *Glob. Biogeochem.* 32, 1542–1555. Cycles. doi:10.1029/2018GB005974

Richardson, J. B., Friedland, A. J., Engerbretson, T. R., Kaste, J. M., and Jackson, B. P. (2013). Spatial and Vertical Distribution of Mercury in Upland Forest Soils across the Northeastern United States. *Environ. Pollut.* 182, 127–134. doi:10.1016/j.envpol.2013.07.011

Richardson, J. B. (2022). Shale Weathering Profiles Show Hg Sequestration along a New York–Tennessee Transect. *Environ. Geochem. Health* 44, 3515–3526. doi:10.1007/s10653-021-01110-x

Roulet, M., Lucotte, M., Saint-Aubin, A., Tran, S., Rhéault, I., Farella, N., et al. (1998). The Geochemistry of Mercury in Central Amazonian Soils Developed on the Alter-Do-Chão Formation of the Lower Tapajós River Valley, Pará State, Brazil1The Present Investigation Is Part of an Ongoing Study, the CARUSO Project (IDRC-UFPa-UQAM), Initiated to Determine the Sources, Fate, and Health Effects of MeHg in the Lower Tapajós area.1. *Sci. Total Environ.* 223, 1–24. doi:10.1016/s0048-9697(98)00265-4

Schroeder, W. H., and Munthe, J. (1998). Atmospheric Mercury - an Overview. *Atmos. Environ.* 32, 809–822. doi:10.1016/S1352-2310(97)00293-8

Schuster, P. F., Schaefer, K. M., Aiken, G. R., Antweiler, R. C., Dewild, J. F., Gryziec, J. D., et al. (2018). Permafrost Stores a Globally Significant Amount of Mercury. *Geophys. Res. Lett.* 45, 1463–1471. doi:10.1002/2017GL075571

SECS-SLCS-IEC (2023). Diccionario Multilingüe de la Ciencia del Suelo, español, catalán, gallego y portugués, con equivalencias en francés e inglés. Available from: https://cit.iec.cat/DiccMCS/inici.html (Accessed February 27, 2023).

Skyllberg, U., Bloom, P. R., Qian, J., Lin, C., and Bleam, W. F. (2006). Complexation of Mercury(II) in Soil Organic Matter: EXAFS Evidence for Linear Two-Coordination with Reduced Sulfur Groups. *Environ. Sci. Technol.* 40, 4174–4180. doi:10.1021/es0600577

Smith-Downey, N. V., Sunderland, E. M., and Jacob, D. J. (2010). Anthropogenic Impacts on Global Storage and Emissions of Mercury from Terrestrial Soils:

Insights from a New Global Model. *J. Geophys. Res. G. Biogeosci.* 115, G03008. doi:10.1029/2009JG001124

Spinola, D., Portes, R., Fedenko, J., Lybrand, R., Dere, A., Biles, F., et al. (2022). Lithological Controls on Soil Geochemistry and Clay Mineralogy across Spodosols in the Coastal Temperate Rainforest of Southeast Alaska. *Geoderma* 428, 116211. doi:10.1016/j.geoderma.2022.116211

Taboada Castro, M. T., Ramil Rego, P., and Díaz-Fierros, F. (1995). *Formación de suelos policíclicos durante el Cuaternario reciente en el Monte Borrelho (N. de Portugal)*, 20. Cuadernos del Laboratorio Xeolóxico de Laxe, 27–36.

Tipping, E., Lofts, S., Hooper, H., Frey, B., Spurgeon, D., and Svendsen, C. (2010). Critical Limits for Hg(II) in Soils, Derived from Chronic Toxicity Data. *Environ. Pollut.* 158, 2465–2471. doi:10.1016/j.envpol.2010.03.027

Urrutia, M., Macías, M., and García-Rodeja, E. (1995). Evaluación del $CuCl_2$ y del $LaCl_3$ como extractantes de aluminio en suelos ácidos de Galicia. *Nova Acta Cient. Compostelana* 5, 173–182.

Wang, X., Luo, J., Yin, R., Yuan, W., Lin, C. J., Sommar, J., et al. (2017). Using Mercury Isotopes to Understand Mercury Accumulation in the Montane Forest Floor of the Eastern Tibetan Plateau. *Environ. Sci. Technol.* 51, 801–809. doi:10.1021/acs.est.6b03806

Xin, M., and Gustin, M. S. (2007). Gaseous Elemental Mercury Exchange with Low Mercury Containing Soils: Investigation of Controlling Factors. *Appl. Geochem.* 22, 1451–1466. doi:10.1016/j.apgeochem.2007.02.006

Zhou, J., Du, B., Shang, L., Wang, Z., Cui, H., Fan, X., et al. (2020). Mercury Fluxes, Budgets, and Pools in Forest Ecosystems of China: A Review. *Crit. Rev. Environ. Sci. Technol.* 50, 1411–1450. doi:10.1080/10643389.2019.1661176

Zhou, J., Wang, Z., Zhang, X., and Gao, Y. (2017). Mercury Concentrations and Pools in Four Adjacent Coniferous and Deciduous Upland Forests in Beijing, China. *J. Geophys. Res. Biogeosci.* 112, 1260–1274. doi:10.1002/2017JG003776

Copyright © 2023 Gómez-Armesto, Méndez-López, Parente-Sendín, Calvo-Portela, Pontevedra-Pombal, García-Rodeja, Alonso-Vega and Nóvoa-Muñoz. This is an open-access article distributed under the terms of the Creative Commons Attribution License (CC BY). The use, distribution or reproduction in other forums is permitted, provided the original author(s) and the copyright owner(s) are credited and that the original publication in this journal is cited, in accordance with accepted academic practice. No use, distribution or reproduction is permitted which does not comply with these terms.